Int. J. Solids Structures, 1970, Vol. 6, pp. 809 to 827. Pergamon Press. Printed in Great Britain

MODE APPROXIMATIONS FOR RIGID–PLASTIC STRUCTURES SUPPORTED BY AN ELASTIC MEDIUM

GIULIANO AUGUSTI†

Brown University, Providence, Rhode Island

Abstract—A rational procedure for obtaining simple approximations of the displacement fields is developed for the structures in the title, loaded statically beyond the point at which plastic flow begins. Some examples, pertaining to beams and plates on Winkler soil (or heavy liquid), illustrate the procedure.

1. NOTATION

$B = B(\xi)$, $F = F(\xi)$, $G = G(\xi)$	auxiliary functions [Example (a)]
b	position of hinges (or hinge circle) in approximate displacement fields u^*
c_i, c	reaction constants
l	half-length of beam (Figs. 2 and 4)
M	bending moment
M^*	statically admissible moments
M_0	(positive) full-yield (or *limit*) bending moment
M_r, M_θ	radial and tangential bending moments in plate
P	applied force (reference value)
q_j, Q_j	generalized strains and stresses
q_j^*	strain in approximate solution
Q_j^*	statically admissible stresses in approximate solution
Q_j'	kinematically admissible stresses in approximate solution
R	plate radius [Example (c)]
r	current radius [Example (c)]
S	surface of body Ω
u_i, u	displacements
u_i^*, u^*	displacements in approximate solution
$\mathbf{x}$	position vector
W^*	strain energy of supporting medium, in approximate solution
Γ	see equation (10)
Δ, Δ^+	see equations (9) and (12)
Δ_m	value of Δ^+ for $\xi = \xi_m$
η_i, η_i^*	characteristic values of u and u^* (Examples)
μ	ratio of negative to positive limit moment of plate (Fig. 7)
ξ	load factor
ξ_1	*threshold* factor (formation of plastic mechanism)
ξ_2	other characteristic value of ξ
ξ_m	maximum value of ξ for a given loading program
ρ	ratio Δ^+/W^*
ρ_m	value of ρ for $\xi = \xi_m$
$\phi(Q_j)$	yield function
Ω	rigid–perfectly plastic body (Fig. 1)
$(\dot{\ })$	$\dfrac{\partial}{\partial \xi}(\ )$
$\langle(\ )\rangle$	$\begin{cases} = 0 & \text{when } (\ ) < 0 \\ = 1 & \text{when } (\ ) = 0 \end{cases}$
$(\ )_i \cdot (\ )_i$	$\sum_1^3 {}_i(\ )_i(\ )_i$

† On leave of absence from the School of Engineering, Università di Napoli, Italy.

2. INTRODUCTION

A NUMBER of important structures, such as platforms floating on heavy liquid and foundation beams or slabs on comparatively soft soil, are supported by continuously distributed reactions, whose unit value increases more or less proportionally with the increase of the corresponding displacements.

If one tries and applies the theory of plastic structures to such instances, it is found that, under quasi-statically increasing applied forces, a *plastic mechanism* develops in the structure at a certain *threshold* load intensity: thereafter (even if second-order geometry effects are neglected), the external forces can continue to increase, essentially because the supporting reactions also increase. Therefore, the *threshold* load is essentially different from the *collapse* or *limit* load defined in the usual simple plastic theory.

As the applied forces increase beyond the threshold value, in general, the changing pattern of loading causes the shape of the incremental displacement field to change also: in other words (in the language appropriate to one- and two-dimensional structures) the plastic hinges *travel* during the loading process. Although this phenomenon has been recognized for some time [1], rather little progress appears to have been made along this line, probably because of the great mathematical difficulties involved in following the changing displacement patterns of even the simplest examples, coupled with the physically unacceptable result of loads that can increase beyond any limit. However, problems of this type had to be solved for practical purposes: indeed [2] "the rapid expansion of airports and the increase in the weight of modern aircraft, as well as the growth of highway traffic, requires the design of more and thicker pavements for heavy wheel loads and great traffic volumes" (1962). Different authors have tackled the problem in different ways: either by developing semi-empirical formulae for the *ultimate load* fitting the results of experiments (e.g. [3]), or by calculating the *collapse load* according to the simple plastic theory of limit analysis but neglecting the variation of support reaction with displacement [4, 2], or by assuming that the unit soil reaction has a well-defined yield limit, so that a *collapse* situation of the structure-soil complex is eventually reached [5, 6].

On the other hand, *traveling hinges* have long been known to occur in dynamically loaded plastic structures (see e.g. [7–9]). In this field of research, theorems have been established [10–12] which allow, in most cases, to find very simple approximate solutions, with a measurable degree of overall approximation.

In the present paper, similar theorems are derived for statically-loaded, rigid–plastic structures embedded in an elastic medium. It is thus possible to develop a very simple procedure for finding approximate displacement fields, whose degree of approximation is known or at least bounded: it is felt that in this way not only it is possible to analyze the overall performance, for example, of a foundation slab on an elastic soil, but also to introduce more rational criteria for the failure of the soil itself, based on the deformation over a finite area rather than on the stress values at each point independently of the neighboring ones.

Some examples illustrate the problem and the suggested procedure.

3. DEFINITION OF THE PROBLEM

Consider a rigid–perfectly plastic body Ω subjected to forces ξP_n, which increase quasi-statically in proportion to a single parameter ξ (Fig. 1). Part S of the surface of Ω is *embedded*

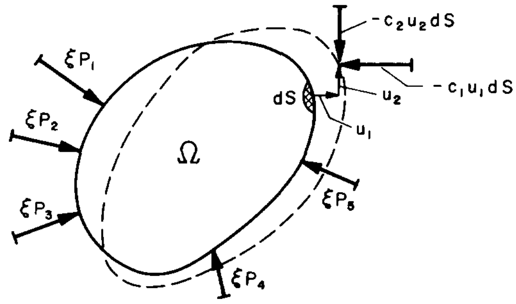

FIG. 1. Diagram of general body in elastic medium.

in an elastic medium, i.e. is subjected to distributed reactions, of componenents $-c_iu_i$/unit surface, where u_i are the cartesian components of the displacement of each point of S and c_i are non-negative *reaction coefficients* ($i = 1, 2, 3$). It is assumed that the c_i's may vary from point to point but are constant with respect to ξ, and that the reactions $-c_iu_i\,\mathrm{d}S$ are able to equilibrate the loads ξP_n.

The displacement, generalized strain and generalized stress fields in Ω will be indicated by $u_i(\mathbf{x}, \xi)$, $q_j(\mathbf{x}, \xi)$, $Q_j(\mathbf{x}, \xi)$ respectively, where $\mathbf{x}$ is the position vector. The variation in the strain field for an increment $\mathrm{d}\xi$ of ξ is related to the (instantaneous) stress field by the plastic flow rule

$$\dot{q}_j(\mathbf{x}, \xi) = \lambda\langle\phi(Q_j)\rangle\frac{\partial\phi(Q_j)}{\partial Q_j}. \tag{1}$$

Here, as in the following, a superimposed dot indicates differentiation with respect to ξ; λ is an arbitrary non-negative constant;

$$\langle\phi(Q_j)\rangle = \begin{cases} 0 & \text{when} \quad \phi(Q_j) < 0 \\ 1 & \text{when} \quad \phi(Q_j) = 0 \end{cases} \tag{2}$$

and $\phi(Q_j)$ is the yield function of the material: states of stress such that $\phi(Q_j) > 0$ are excluded. Again, the function $\phi(Q_j)$ is permitted to vary with $\mathbf{x}$ but not with ξ.

Under these assumptions, as long as the load factor remains in the interval

$$0 \leqslant \xi \leqslant \xi_1 \tag{3}$$

the strain field is everywhere nil and the displacement field u_i corresponds to a rigid-body motion. When ξ reaches the value ξ_1 (which will be referred to as the *threshold value*), the stress field allows, through equation (1), a compatible set of strain increments: in other words, a *plastic mechanism* has formed and the rigid–plastic body begins deforming. The displacement increments are uniquely related to the strain increments, to within a rigid-body motion which is determined by equilibrium.

As ξ increases further, the stress field changes, due to the change in the displacement and reaction fields, and in general the strain and displacement-increment fields change too: in other words, the displacement field varies with ξ not only in magnitude but also in shape, just like in impulsive load problems it varies with time. Its determination does not offer any conceptual difficulty, but calls for great computational work: therefore, it may be worth looking for an approximate solution, which is indeed the object of this paper.

4. CONSTRUCTION OF AN APPROXIMATE DISPLACEMENT FIELD

Consider a displacement field $u_i^*(\mathbf{x}, \xi)$, such that the reactions $-c_i u_i^* \, \mathrm{d}S$ are in equilibrium with loads ξP_n, but otherwise arbitrary: this field will be taken as an approximate solution for the displacements $u_i(\mathbf{x}, \xi)$. In practical applications, it will be often convenient to choose a field u_i^* such that its *shape* does not vary with time, i.e. a *mode approximation*

$$u_i^*(\mathbf{x}, \xi) = v_i(\mathbf{x}) f(\xi). \tag{4}$$

However, the arguments in this section are not limited to fields of the type (4); only fields with moving discontinuities of u_i^* are excluded.

Let $\dot{q}_j^*$ be the strain increments determined by u_i^*, and Q_j' the stresses associated with any non-zero $\dot{q}_j^*$ by the plastic flow rule (1). Assume also that, for any relevant value of ξ, a stress field Q_j^* can be found throughout Ω, in equilibrium with ξP_n and $-c_i u_i^* \, \mathrm{d}S$, and not violating the yield condition

$$\phi(Q_j^*) \leqslant 0. \tag{5}$$

The stresses $(Q_j - Q_j^*)$ are in equilibrium with zero external forces and surface reactions $-c_i(u_i - u_i^*)$. Applying the principle of virtual work to the above loads and the increment of $(u_i - u_i^*)$ for an infinitesimal variation of ξ,

$$-\int_S c_i(u_i - u_i^*) \cdot (\dot{u}_i - \dot{u}_i^*) \, \mathrm{d}S = \int_\Omega (Q_j - Q_j^*) \cdot (\dot{q}_j - \dot{q}_j^*) \, \mathrm{d}\Omega. \tag{6}$$

Since Q_j and $\dot{q}_j$ are associated through the flow rule and Q_j^* satisfies the yield condition (5), Drucker's stability postulate [10, 13] yields

$$\int_\Omega (Q_j - Q_j^*) \cdot \dot{q}_j \, \mathrm{d}\Omega \geqslant 0 \tag{7'}$$

and for analogous reasons

$$\int_\Omega (Q_j' - Q_j) \cdot \dot{q}_j^* \, \mathrm{d}\Omega \geqslant 0 \tag{7''}$$

whence, after some algebra

$$\int_\Omega (Q_j - Q_j^*) \cdot (\dot{q}_j - \dot{q}_j^*) \, \mathrm{d}\Omega \geqslant -\int_\Omega (Q_j' - Q_j^*) \cdot \dot{q}_j^* \, \mathrm{d}\Omega. \tag{8}$$

Let now

$$\Delta = \frac{1}{2} \int_S c_i(u_i - u_i^*) \cdot (u_i - u_i^*) \, \mathrm{d}S \tag{9}$$

$$\Gamma = \int_\Omega (Q_j' - Q_j^*) \cdot \dot{q}_j^* \, \mathrm{d}\Omega \tag{10}$$

Δ is a positive-definite quantity, that can be taken as an overall measure of the difference between the approximate displacement field u_i^* and the exact field u_i; Γ is also a non-negative quantity which depends only on the approximate field u_i^* and its variation with ξ.

Introducing (8), (9) and (10), equation (6) becomes

$$\frac{\partial \Delta}{\partial \xi} \leqslant \Gamma. \tag{11}$$

Initially (i.e. for $\xi = 0$) both fields u_i and u_i^* are identically zero; therefore inequality (11) can be integrated to give an upper bound on Δ for any value of ξ, in the form

$$\Delta(\xi) \leqslant \Delta^+(\xi) = \int_0^{\xi} \Gamma \, \mathrm{d}\xi \tag{12}$$

$\Delta^+(\xi)$ is thus an upper bound to a measure of the overall approximation involved in substituting u_i^* to u_i: it is given by quantities related to the approximate field u_i^* only, and therefore can be calculated once u_i^* is known. The only condition for the validity of this upper bound is that a statically admissible field Q_j^* can be determined in conjunction with u_j^*: however, it will be seen in Example (a) that this condition can be relaxed in some special cases of practical interest.

In order to evaluate the quantitative meaning of Δ^+, it should be compared with some other analogous quantity, either known *a priori* or depending on u_i^* only. For instance, such a quantity is the elastic energy stored in the embedding medium

$$W^* = \frac{1}{2}\int_S c_i u_i^* \, . \, u_i^* \, \mathrm{d}S. \tag{13}$$

It seems fair to assume that in general the approximate field u_i^* is the more reliable, the smaller is the ratio

$$\rho = \frac{\Delta^+}{W^*}. \tag{14}$$

However, since also W^* actually depends on u_i^*, this statement must not be taken to be too restrictive: for instance, if more than one field u_i^* can be found, the most reliable is the one with smallest Δ^+, and not ρ.

5. EXAMPLES

(a) *Beam under two end forces* (*Fig.* 2)

Let $2l$ be the length of a rigid–plastic beam, loaded at the ends by two equal downward forces ξP and supported on an elastic soil whose reaction/unit length of beam is equal to $-cu$, where u is the displacement of the beam (positive downwards). This beam goes through three phases of behavior, as the load factor ξ increases:

Phase I ($0 \leqslant \xi \leqslant \xi_1$). The beam moves rigidly downwards [Fig. 2(a)], with a constant displacement $u = \eta_1$ given by equilibrium

$$\eta_1 = \xi \frac{P}{cl}. \tag{a1}$$

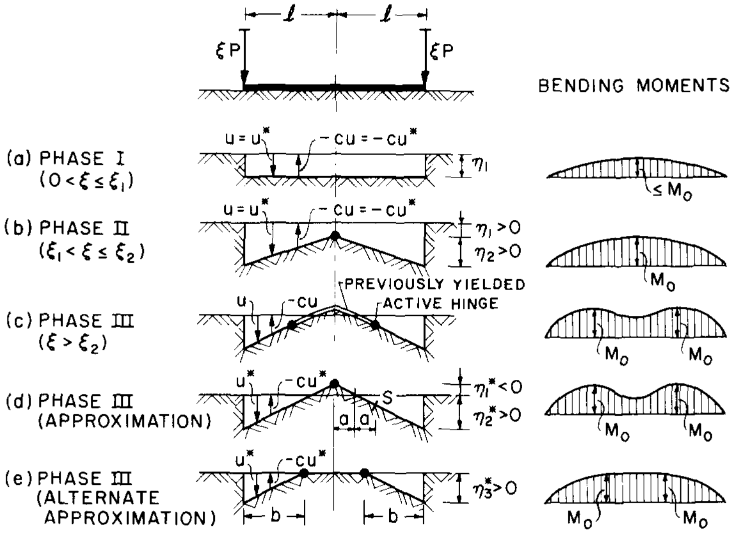

FIG. 2. Example (a).

The maximum moment occurs in the mid-span section B, and is equal to

$$M_B = c\eta_1\frac{l^2}{2} = \xi P\frac{l}{2} \tag{a2}$$

(Hogging bending moments are taken as positive in this example.) The *threshold* value of ξ is given by

$$M_B = M_0 = \xi_1 P\frac{l}{2}, \quad \text{i.e. } \xi_1 = \frac{2M_0}{Pl} \tag{a3}$$

where M_0 is the (hogging) limit moment of the beam. Choosing the reference value P such that

$$M_0 = P\frac{l}{2} \tag{a4}$$

the *threshold* load factor is

$$\xi_1 = 1 \tag{a5}$$

Phase II ($\xi_1 < \xi \leqslant \xi_2$). As soon as $\xi > \xi_1$, plastic rotations take place in the *plastic hinge B* [Fig. 2(b)]. Overall equilibrium gives

$$\eta_1 + \frac{1}{2}\eta_2 = \xi\frac{P}{cl} \tag{a6}$$

and the yield condition

$$M_0 = \xi Pl - c\eta_1\frac{l^2}{2} - c\eta_1\frac{l^2}{3}. \tag{a7}$$

Introducing (a4), equations (a6) and (a7) give

$$\eta_1 = \frac{2M_0}{cl^2}(3 - 2\xi)$$
$$\eta_2 = \frac{2M_0}{cl^2}6(\xi - 1). \tag{a8}$$

The deformation of the beam remains concentrated in the only plastic hinge in B as long as B is the maximum moment section, i.e. as long as

$$\eta_1 \geqslant 0, \quad \text{or} \quad \xi \leqslant \xi_2 = \frac{3}{2}. \tag{a9}$$

Phase III ($\xi > \xi_2$). In this phase, $u < 0$ in the central portion of the beam, that is therefore loaded by a downward reaction: B is no more the maximum moment section, and the plastic hinge splits in two symmetric hinges which move steadily towards the ends of the beam as ξ increases [Fig. 2(c)]. An approximate solution u^* is assumed in this phase, such that the plastic rotation remains concentrated in B [Fig. 2(d)].

The general treatment shows that the bound Δ^+ holds for this approximation as long as a bending moment diagram M^* can be found, in equilibrium with loads ξP and reactions $-cu^*$, and satisfying the yield condition. Note however that the validity of inequality (7′) is the only reason for which M^* is required not to violate the yield condition: in this particular example one can easily argue that the true rate of curvature is always non-negative, so that

$$M^* \leqslant M_0 \tag{a10}$$

is a sufficient condition for validity of (7′), and therefore is the only limitation which will be imposed to the approximate field u^*.

Overall equilibrium yields the same equation (a6) of Phase II. The shear force is zero, i.e. M^* is maximum, in sections S at a distance $2a$ from B, where [Fig. 2(c)]

$$a = \frac{-\eta_1^*}{\eta_2^*}l. \tag{a11}$$

Equating to M_0 the bending moment in S

$$M_0 = \xi P(l - 2a) - c\left(\eta_1^* + \frac{2a}{l}\eta_2^*\right)\frac{(l-2a)^2}{2} - c\frac{l-2a}{l}\eta_2^*\frac{(l-2a)^2}{3}. \tag{a12}$$

Equations (a4), (a6), (a11) and (a12), after some algebra, give

$$\eta_1^* = \frac{2M_0}{cl^2}\left\{\xi - \frac{\xi^2}{2}\left[1 + \sqrt{\left(1 - \frac{4}{3\xi}\right)}\right]\right\}$$
$$\eta_2^* = \frac{2M_0}{cl^2}\xi^2\left[1 + \sqrt{\left(1 - \frac{4}{3\xi}\right)}\right]. \tag{a13}$$

The diagrams of η_1, η_2, η_1^*, η_2^*, as obtained from equations (a1), (a8) and (a13), are plotted in Fig. 3(a).

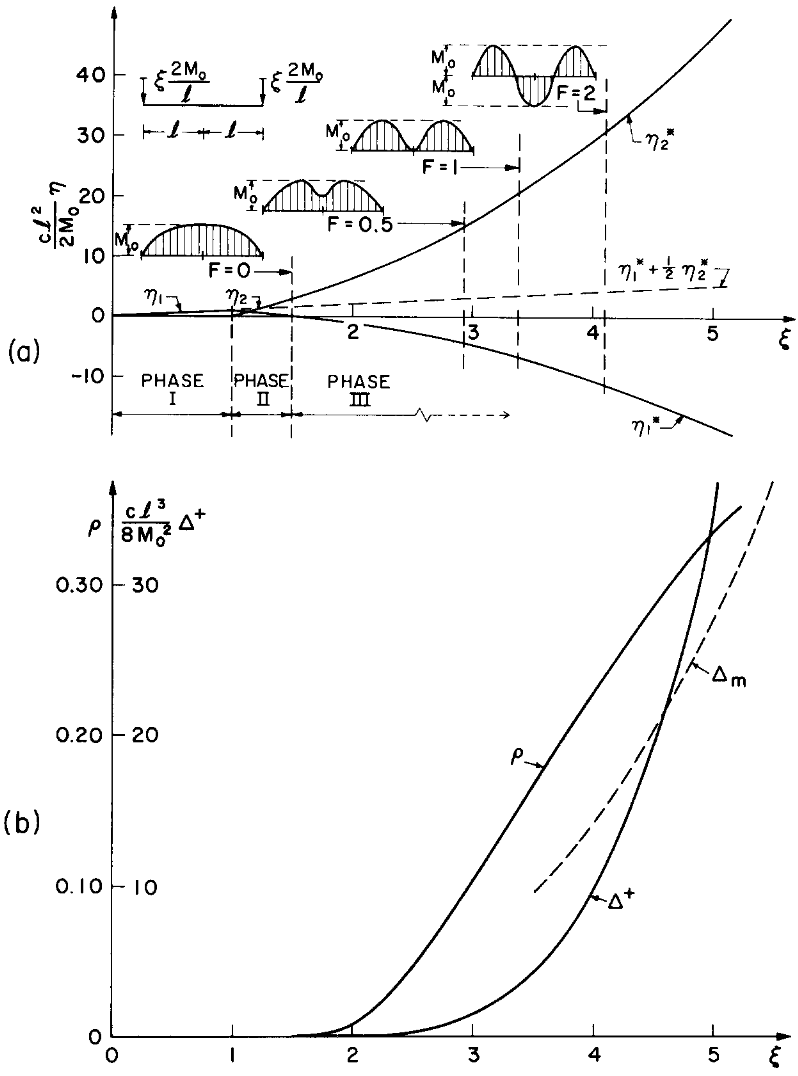

FIG. 3. Example (a): Approximate displacements and measure of approximation.

The bending moment in B is

$$M_B^* = \xi Pl - c\eta_1^* \frac{l^2}{2} - c\eta_2^* \frac{l^2}{3}. \tag{a14}$$

Introduction of (a4) and (a13) into (a14) leads easily to

$$\frac{M_0 - M_B^*}{M_0} = 1 - \xi + \frac{\xi^2}{6}\left[1 + \sqrt{\left(1 - \frac{4}{3\xi}\right)}\right] = F(\xi). \tag{a15}$$

Some successive moment diagrams M^*, with the corresponding values of F, are sketched in Fig. 3(a). Note that when $F > 2$ (i.e. $\xi > 4{\cdot}1$ approx.), the M^* diagram violates the yield condition, because $M_B^* < -M_0$: however, inequality (a10) holds.

In the present example, equation (10) becomes

$$\Gamma = (M_0 - M_B^*)\frac{2\dot{\eta}_2^*}{l}. \tag{a16}$$

The second equation (a13) gives

$$\dot{\eta}_2^* = \frac{2M_0}{cl^2}\left[\xi + \frac{\xi - 1}{\sqrt{\left(1 - \frac{4}{3\xi}\right)}}\right] = \frac{4M_0}{cl^2}G(\xi). \tag{a17}$$

Introducing (a15), (a16) and (a17) into (12), one gets

$$\begin{aligned} \Delta^+ &= 0 \qquad \text{for} \quad 0 \leqslant \xi \leqslant \tfrac{3}{2} \\ \Delta^+ &= \frac{8M_0^2}{cl^3}\int_{\frac{3}{2}}^{\xi} FG\,\mathrm{d}\xi \quad \text{for} \quad \xi \geqslant \tfrac{3}{2}. \end{aligned} \tag{a18}$$

Equation (13), with introduction of (a13), becomes

$$W^* = \int_0^l c\left(\eta_1^* + \eta_2^*\frac{z}{l}\right)^2 \mathrm{d}z = \frac{4M_0^2}{cl^3}B(\xi) \tag{a19}$$

where

$$B(\xi) = \xi^2\left\{1 + \frac{\xi^2}{12}\left[1 + \sqrt{\left(1 - \frac{4}{3\xi}\right)}\right]^2\right\}. \tag{a20}$$

In turn, equation (14) yields

$$\rho = \frac{\Delta^+}{W^*} = 2\frac{\int_{\frac{3}{2}}^{\xi} FG\,\mathrm{d}\xi}{B} \qquad (\xi \geqslant \tfrac{3}{2}). \tag{a21}$$

Equations (a19) and (a21) are plotted in Fig. 3(b). It can be noted that they guarantee that the approximation u^* is reasonably good up to loads 4 or $4\frac{1}{2}$ times the threshold value $\xi_1 = 1$.

However, if the maximum load $\xi_m P$ is larger, it may be more convenient to choose another displacement field, for instance one like in Fig. 2(e). In this case, equilibrium requires

$$\xi P = \tfrac{1}{2}cb\eta_3^*. \tag{a22}$$

The bending moment M^* is constant between sections D and E, and equal to

$$M_{DE}^* = \frac{1}{3}\xi P b = \frac{2M_0}{3l}\xi b. \tag{a23}$$

Inequality (a10) holds if

$$b \leqslant \frac{3l}{2\xi_m} \tag{a24}$$

where ξ_m is the maximum value reached by ξ. Equation (10) becomes, with introduction of (a22) and (a23),

$$\Gamma = 2(M_0 - M_{DE}^*)\frac{\dot{\eta}_3^*}{b} = \frac{8M_0}{clb^2}\left(1 - \frac{2}{3}\frac{b}{l}\xi\right). \tag{a25}$$

It is evident that, for any loading program, the best approximation is obtained if the largest possible b is chosen: i.e. if the equality sign is introduced in (a24).

The final value of Δ^+ is then given by

$$\Delta_m = \Delta^+(\xi_m) = \int_0^{\xi_m} \Gamma\, d\xi = \frac{8M_0}{cl^3}\left(\frac{2\xi_m}{3}\right)^2 \int_0^{\xi_m}\left(1 - \frac{\xi}{\xi_m}\right) d\xi = \frac{8M_0}{cl^3}\cdot\frac{2\xi_m^3}{9}. \tag{a26}$$

Equation (a26) is plotted as a broken line in Fig. 3(b). It can thus be noted that, with the optimum choice of b, the mode approximation in Fig. 2(e) is more reliable than that in Fig. 2(d) when ξ_m is larger than 4·55 approx.

(b) *Infinite beam under single concentrated force*

The infinitely long beam will be studied as the limit case of the beam in Fig. 4. Also this beam goes through three phases while ξ increases:

Phase I ($0 \leq \xi \leq \xi_1$). The beam moves rigidly downwards, of a quantity η_1 given by

$$\xi P = 2c\eta_1 l. \tag{b1}$$

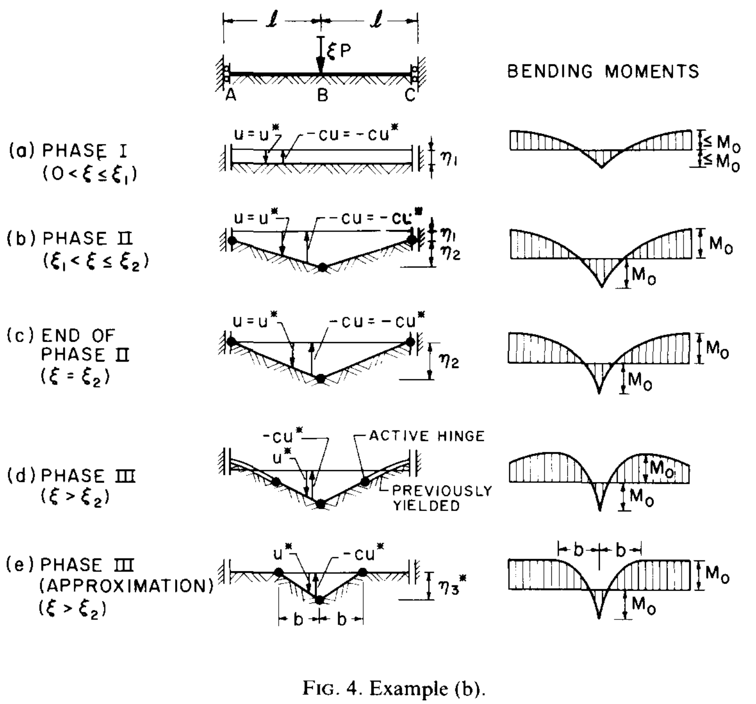

FIG. 4. Example (b).

Assuming that the positive and negative yield moments of the beam section are equal and taking the sagging moments as positive, the threshold load $\xi_1 P$ corresponds to

$$\begin{aligned} M_B &= +M_0 \\ M_A = M_c &= -M_0 \end{aligned} \tag{b2}$$

i.e. to

$$2M_0 = \xi_1 P \frac{l}{4}, \quad \text{i.e.} \quad \xi_1 = \frac{8M_0}{Pl}. \tag{b3}$$

Phase II ($\xi_1 < \xi \leqslant \xi_2$). The beam deforms with three plastic hinges, as indicated in Fig. 4(b). As in the previous example, the end of this phase is reached when η_1 vanishes, i.e. [Fig. 4(c)] when

$$2M_0 + \xi_2 P \frac{l}{6}, \quad \text{i.e.} \quad \xi_2 = \frac{3}{2}\xi_1. \tag{b4}$$

Phase III ($\xi > \xi_2$). The central plastic hinge remains stationary in B, the two lateral ones move towards the center of the beam: the displacements at a certain stage look like in Fig. 4(d). Operating as described with reference to Fig. 2(e), one can assume the approximate field u^* in Fig. 4(e) with

$$b \leqslant \frac{12M_0}{\xi_m P} \tag{b5}$$

Taking the equality sign in (b5), and applying formulae already used, it is easy to derive the final values of η_3^*, Δ^+, W^* and ρ for any prescribed value of ξ_m

$$\eta_m^* = \eta_3^*(\xi_m) = \frac{(\xi_m P)^2}{12cM_0} \tag{b6}$$

$$\Delta_m = \Delta^+(\xi_m) = \frac{(\xi_m P)^2}{72cM_0} \tag{b7}$$

$$W_m = W^*(\xi_m) = \frac{(\xi_m P)^3}{36cM_0} \tag{b8}$$

$$\rho_m = \frac{\Delta_m}{W_m} = 0{\cdot}5. \tag{b9}$$

It is of interest to note that ρ_m is independent of ξ_m.

Infinite beam. Equations (b3) and (b4) show that

$$\lim_{l\to\infty} \xi_0 = \lim_{l\to\infty} \xi_1 = 0. \tag{b10}$$

Therefore, Phases I and II disappear completely for the infinitely long rigid–plastic beam: for any non-zero load three plastic hinges are active, one directly under the force ξP, and two traveling continuously towards the loaded section. A mode approximation should be applied from the beginning of the loading: the one described with reference to Fig. 4(e) is perfectly appropriate, and the relevant equations (b5–9) fully valid.

There is no limit to the maximum force $\xi_m P$ that the beam is able to carry under the present assumptions. For any ξ_m, the best approximation is obtained with b as given by (b5) with the equality sign. Once b has been chosen, η_3^* increases linearly with the load (Fig. 5); the final value of η_3^*, η_m^*, is as given by equation (b6).

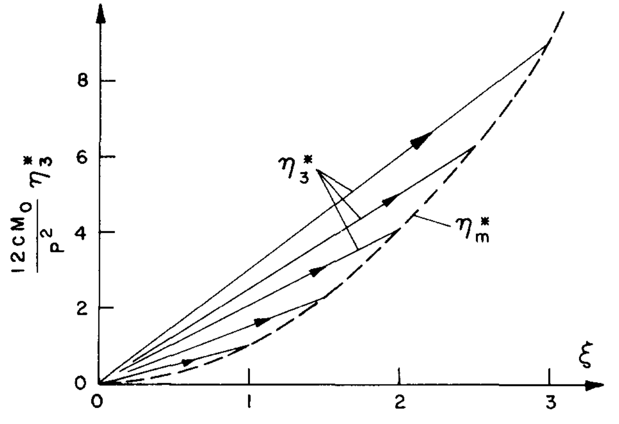

FIG. 5. Example (b) ($l = \infty$): Approximate central displacements.

(c) *Infinite plate under single load*

Similar to example (b), the infinite plate will be studied as the limit case of the circular plate in Fig. 6.

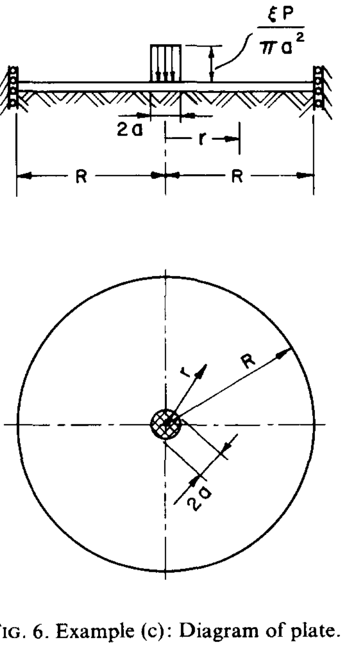

FIG. 6. Example (c): Diagram of plate.

The external load ξP is applied as a uniform pressure over a small circle of radius $a \ll R$, concentric with the plate; the square yield criterion in Fig. 7 is assumed to hold for the plate. The positive moments and shear forces acting on plate element are defined in Fig. 8; the supporting reaction is equal to $-cu$ per unit surface, where μ is the downward displacement and c is constant.

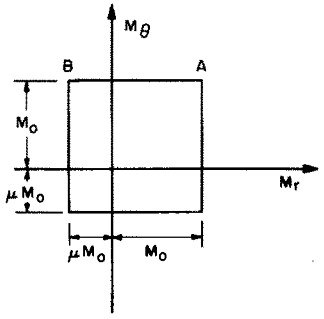

FIG. 7. Yield locus of plate.

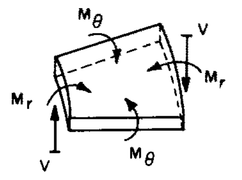

FIG. 8. Positive (generalized) stresses.

In the development of the example, we shall be concerned only with stress states such that the shear force is zero along a circumference of radius r_1, and the circumferential bending moment M_θ is constant for $r < r_1$. Therefore, the relevant equations of equilibrium can be directly written with reference to the elementary "slice" of plate in Fig. 9, and are

$$\xi P = 2\pi c \int_0^{r_1} ur \, \mathrm{d}r \tag{c1}$$

$$\xi P(r_g - \tfrac{2}{3}a) - 2\pi r_1(M_\theta - M_{r1}) = 0 \tag{c2}$$

where

$$r_g = \frac{\displaystyle\int_0^{r_1} ur^2 \, \mathrm{d}r}{\displaystyle\int_0^{r_1} ur \, \mathrm{d}r} \tag{c3}$$

and

$$M_{r_1} = M_r|_{r=r_1}. \tag{c4}$$

The plate goes through three phases of behavior similar to those in Fig. 4.

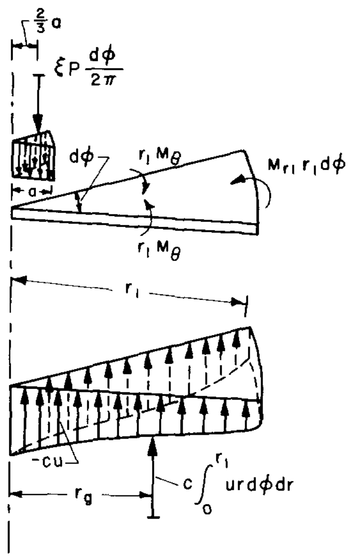

FIG. 9. Elementary "slice" of plate.

Phase I ($0 \leqslant \xi \leqslant \xi_1$). The plate moves rigidly downwards; u is constant and equal to η_1, say, and $r_1 = R$ [Fig. 10(a)]. The equations of equilibrium (c1) and (c2) become

$$\xi P = \pi R^2 c \eta_1 \tag{c5}$$

$$\tfrac{2}{3}\xi P(R - a) - 2\pi R(M_\theta - M_{r1}) = 0. \tag{c6}$$

The limit of Phase I is reached when

$$\begin{aligned} M_\theta = M_r|_{r=0} &= +M_0 \\ M_r|_{r=R} = M_{r1} &= -\mu M_0. \end{aligned} \tag{c7}$$

Introducing (c7) into (c6), the *threshold load factor* ξ_1 is obtained

$$\xi_1 = 3\pi(1 + \mu)\frac{M_0}{P}\frac{R}{R - a}. \tag{c8}$$

By choosing the reference value P as follows

$$P = 3\pi(1 + \mu)M_0 \tag{c9}$$

equation (c8) becomes

$$\xi_1 = \frac{R}{R-a}. \tag{c10}$$

Thus, at end of Phase I

$$\eta_1 = \frac{P}{\pi c}\frac{1}{R(R - a)} = 3(1 + \mu)\frac{M_0}{c}\frac{1}{R(R - a)}. \tag{c11}$$

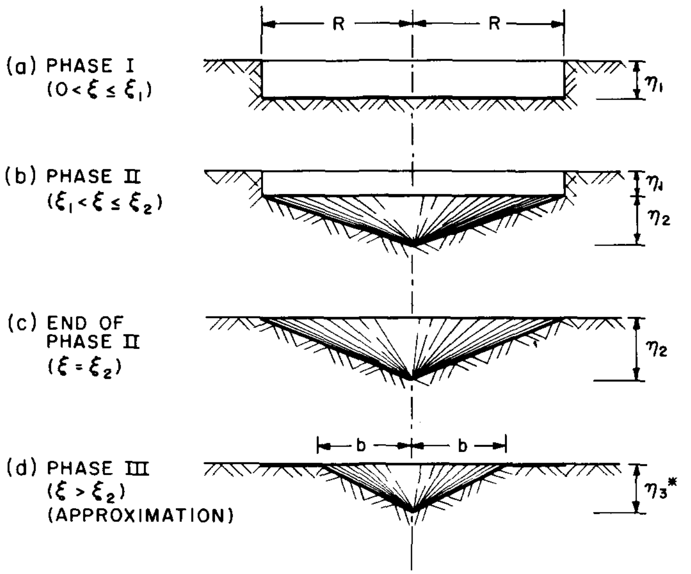

FIG. 10. Example (c): Displacements.

Phase II ($\xi_1 < \xi \leqslant \xi_2$). When equations (c7) hold, the center of the plate is in plastic regime A (Fig. 7), the circumference $r = R$ in regime B, and the rest in regime AB. The displacement field compatible with this stress distribution is a reversed cone, with radius R [Fig. 10(b)]. The end of this phase is reached when the displacement η_1 at $r = R$ vanishes. In this condition [Fig. 10(c)], equations (c3) and (c2) become respectively

$$r_g = \frac{\int_0^R \left(1 - \frac{\eta_2}{R}r\right) r^2 \, dr}{\int_0^R \left(1 - \frac{\eta_2}{R}r\right) r \, dr} = \frac{R}{2} \tag{c12}$$

$$\xi_2 P\left(\frac{R}{2} - \frac{2}{3}a\right) = 2\pi(1 + \mu)RM_0 \tag{c13}$$

and with introduction of (c9)

$$\xi_2 = \frac{R}{\frac{3}{4}R - a}. \tag{c14}$$

It is to be noted that for $\mu = 1$ this value coincides with that given by equation (23) in Ref. [2], and there defined as the *collapse load*.

From equation (c1), the displacement η_2 at end of Phase II is easily obtained.

$$\eta_2 = 3\frac{P}{\pi c}\frac{1}{R(\frac{3}{4}R - a)} = 12(1 + \mu)\frac{M_0}{c}\frac{1}{R(R - \frac{4}{3}a)}. \tag{c15}$$

Phase III ($\xi > \xi_2$). The hinge circle which was located at $r = R$ moves inward and the shape of the deformed plate becomes similar to Fig. 4(d). An approximate solution u^* can be assumed, in the shape of a reversed cone of radius $r_1 = b < R$ [Fig. 10(d)].

A distribution of moments in equilibrium with the loads can be assumed as follows [cf. equations (c12–13)]

$$M_\theta^* = M_r^*|_{r=0} = M_0$$
$$M_r^*|_{r=b} = M_{r1}^* = -\frac{\xi P}{2\pi b}\left(\frac{b}{2} - \frac{2}{3}a\right) + M_0. \tag{c16}$$

These moments satisfy the yield condition if

$$-\mu M_0 \leqslant M_r^*|_{r=b} \leqslant M_0 \tag{c17}$$

for any value of ξ ($0 \leqslant \xi \leqslant \xi_m$). By the same arguments developed with reference to Fig. 4(e), it is then easy to show that the most reliable approximation is obtained with the radius b given by the condition

$$M_r^*|_{r=b} = -\mu M_0 = -\frac{\xi_m P}{2\pi b}\left(\frac{b}{2} - \frac{2}{3}a\right) + M_0 \tag{c18}$$

that is, after introduction of (c9) and some algebra,

$$b = \frac{a}{\dfrac{3}{4} - \dfrac{1}{\xi_m}}. \tag{c19}$$

It is of interest to note (i) that b (c19) decreases from R to $4a/3$ as ξ_m increases from ξ_2 to infinity; (ii) that if $a = 0$ (i.e. if the plate were loaded by a truly concentrated force) no statically admissible bending moment diagram could be found, for $\xi > \xi_2$, with the displacement pattern of Fig. 10(d).

Once b has been fixed, the displacements u^* increase linearly with ξ, according to the equilibrium equation (c1), where $r_1 = b$. In particular, the center displacement η_3^* [Fig. 10(d)] is

$$\eta_3^* = 3\frac{P}{\pi c b^2}\xi = 9(1+\mu)\frac{M_0}{cb^2}\xi. \tag{c20}$$

Introducing $\xi = \xi_m$ and b (c19), the final displacement η_m^* is obtained

$$\eta_m^* = 9(1+\mu)\frac{M_0}{ca^2}\xi_m\left(\frac{3}{4} - \frac{1}{\xi_m}\right)^2. \tag{c21}$$

Equations (c16) and (c20) allow the derivation of Γ

$$\Gamma = 2\pi(\mu M_0 + M_{r1}^*)\dot{\eta}_3^* = 2\pi\frac{[3(1+\mu)M_0]^2}{cb^2}\left(1 - \frac{\xi}{\xi_m}\right) \tag{c22}$$

whence the values of Δ^+, W^*, ρ at the end of the loading

$$\Delta_m = \Delta^+(\xi_m) = \pi[3(1+\mu)M_0]^2 \frac{\xi_m}{ca^2}\left(\frac{3}{4} - \frac{1}{\xi_m}\right)^2 \tag{c23}$$

$$W_m^* = W^*(\xi_m) = \frac{9}{4}\pi[3(1+\mu)M_0]^2 \frac{\xi_m^2}{ca^2}\left(\frac{3}{4} - \frac{1}{\xi_m}\right)^2 \tag{c24}$$

$$\rho_m = \frac{\Delta_m}{W_m^*} = \frac{4}{9\xi_m}. \tag{c25}$$

Infinite Plate ($R = \infty$). As it can be immediately derived from (c14)

$$\lim_{R\to\infty} \xi_1 = 1; \qquad \lim_{R\to\infty} \xi_2 = \tfrac{4}{3} \tag{c26}$$

while (c11) and (c15) yield zero displacements. Therefore, the stress distribution in the infinitely large plate goes through Phases I and II as described, but without any displacement within the relevant approximations.

The description of Phase III and of u^* in Fig. 10(d) is perfectly valid (for $\xi > \xi_2 = \frac{4}{3}$) for the infinite plate. The center displacement η_3^* and Δ_m, ρ_m are therefore as given by equations (c20), (c21) and (c23), (c25) respectively, which are plotted in Fig. 11.

The approximation can be considered satisfactory for any value of ξ_m.

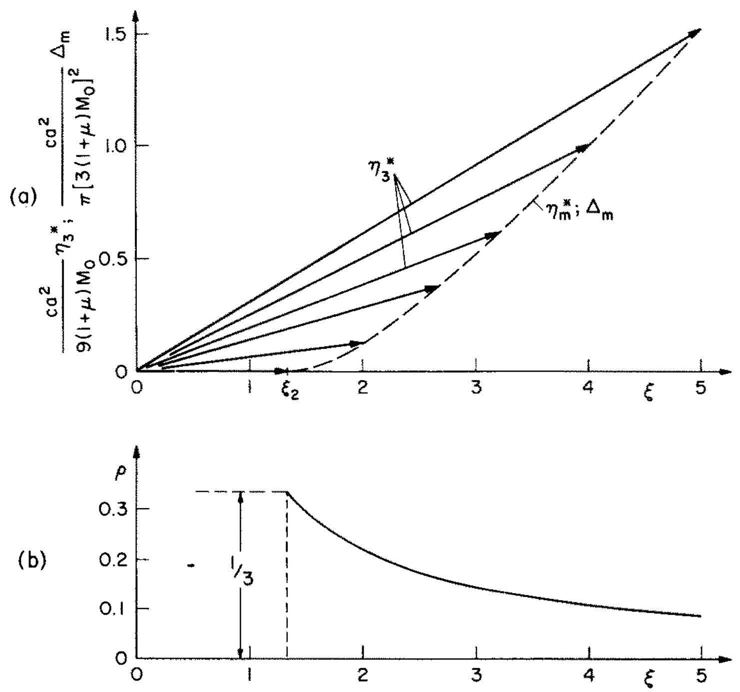

FIG. 11. Example (c) ($R = \infty$): Approximate central displacements and measure of approximation.

6. CONCLUSIONS

In this paper the behavior of rigid–perfectly plastic structures on elastic support has been examined. Some examples have been presented, that can be thought of as representing beams and plates under heavy loads, floating on soft elastic (Winkler) soil or on heavy liquid. The mathematical model of linear dependence between support reaction and displacement, has made it necessary to assume the possibility of reversals in the sign of the reaction, i.e. of *tractions* between structure and support. Physically, this situation arises if the dead weight of the structure can be assimilated to a uniformly distributed load, which does not cause stresses in the structure but gives a permanent constant compressive reaction of sufficient magnitude to maintain contact throughout the loading.

It has been shown that, under quasi-statically increasing loads, plastic hinges are formed in the structure, and then travel with further increase of the loads, generally *towards* the applied forces. Note that on the contrary in impulsive load problems the hinges tend to travel *away* from the points of application of the impulse: however, the hinges may travel in the opposite direction if membrane forces are taken into account (cf. [14] and [15]). The qualitative analogy between membrane forces and continuous elastic reactions is evident: both tend to increase the strength of the structure with the displacements. The analogy in the plastic hinge behavior is therefore quite logical.

It has been shown that the displacements can be approximated by a *mode*, i.e. by a one-degree-of-freedom rigid–plastic mechanism; a rational choice of such mechanism allows a measure of (or at least an upper bound on) the approximation involved. Three examples have been presented, in all of which the approximation appears quite satisfactory.

This simplified approach should allow further treatments of problems of the sort considered here, which are of considerable practical interest, but have so far been rather neglected in the plastic theory of structures.

The analogy with membrane effects might also suggest a possible parallel development in this direction.

Acknowledgement—The research reported in this paper has been supported in part by ARPA through Contract No. SD–86 with Brown University.

REFERENCES

[1] A. R. RJANITSYN, *Calcul à la Rupture et Plasticité des Constructions*, pp. 71–74. (Translated from Russian). Eyrolles (1959).
[2] G. G. MEYERHOF, Load-carrying capacity of concrete pavements, *J. Soil Mech. Found. Div., Am. Soc. Civ. Engrs* **88**, 89–116 (1962).
[3] K. W. JOHANSEN *et al.*, Slabs on Soil, Laboratoriet for Bygningsteknik, Danmarks Tekniske Höjskole, Report No. 4, 1955.
[4] G. G. MEYERHOF Bearing capacity of floating ice sheets, *J. Eng. Mech. Div., Am. Soc. Civ. Engrs* **86**, 113–145 (1960).
[5] A. SAWCZUK and T. JAEGER, *Grenztragfähigkeits-Theorie der Platten*, pp. 186–192. Springer (1963).
[6] G. ZINGONE, Limit analysis of a beam in bending immersed in an elasto–plastic medium, *Meccanica* **3**, 48–56 (1968).
[7] P. S. SYMONDS, Survey of methods of analysis for plastic deformation of structures under dynamic loading, Div. Engng., Brown University, Report BU/NSRDC/1–67 (1967).
[8] H. G. HOPKINS and W. PRAGER, On the dynamics of plastic circular plates, *J. appl. Math. phys.* **5**, 317–330 (1954).
[9] A. L. FLORENCE, Clamped circular rigid–plastic plates under central blast loading, *Int. J. Solids Struct.* **2**, 319–335 (1966).

[10] J. B. Martin and P. S. Symonds, Mode approximations for impulsively-loaded rigid–plastic structures, *J. Engng. Mech. Div., Am. Soc. Civ. Engrs* **92**, 43–66 (1966).
[11] M. A. Oien and J. B. Martin, Approximate methods for rigid–plastic structures subjected to dynamic loading, Div. Engng, Brown University, Report BU/DTMB/7 (1965).
[12] G. Augusti, J. B. Martin and J. D. O'Keeffe, An approximate method of analysis for rigid–plastic pulse-loaded structures. Presented at the *2nd Canadian Congrs. appl. Mech.* Waterloo (1969).
[13] D. C. Drucker, A more fundamental approach to stress–strain relations, *Proc. 1st U.S. Natl. Congr. appl. Mech.* 487 (1951).
[14] N. Jones, Impulsive loading of a simply supported circular plate, Div. of Engng, Brown University, Report ARPA No. 37 (1967).
[15] N. Jones, Finite deflections of a simply supported rigid–plastic circular plate loaded dynamically, Div. of Engng, Brown University, Report ARPA No. E42 (1967).

(*Received* 22 *May* 1969; *revised* 8 *August* 1969)

Абстракт—Выводится рациональный процесс с целью получения приближений полей перемещений для систем, указанных в заглавии, нагруженных статически выше точки, при которой начинается пластическое течение. Некоторые примеры, касающиеся балок и пластиокн на основании Винклера 'или на тяжелой жидкости', иллюстрируют процесс расчета.